Baseband Digital Signal Processing of Radar System

Laura A. Haws[1]

University of New South Wales at the Australian Defence Force Academy

We design and implement a radar system modeled in MATLAB, focusing on fundamental digital signal processing and communication techniques. This implementation will be capable of detecting and displaying multiple radar targets, including its range and azimuth angle from a particular view point on a 'Green Screen' user interface within MATLAB. This project consists of a number of subsections, with each section contributing to the final design of the system. After validation and successful simulation, the sections have been progressively integrated to build a fully operating system incorporating traditional radar techniques in order to fully understand the characteristics and requirements of a radar system. Using this framework, the techniques used in communication systems could possibly be used to build a better radar system and thus the benefits of powerful communication techniques such as CDMA and multiuser detection can start to be exploited in radar.

Contents

[1] PLTOFF, School of Engineering & Information Technology. ZEIT4501

Nomenclature

CDMA	=	code division multiple access
$\emptyset$	=	elevation angle [degrees]
θ	=	azimuth angle [degrees]
3D	=	three-dimensional
PAR	=	phased-array radar
λ	=	wavelength [m]
SNR	=	signal-to-noise ratio
RCS	=	radar cross section
T_x	=	transmitter
R_x	=	receiver
ISI	=	Intersymbol Interference
RCF	=	raised cosine filter
RRC	=	root-raised cosine
ω_c	=	corner frequency [radians/second]
r	=	roll off factor
T_c	=	chip length
H_{RRC}	=	root-raised cosine filter transfer function
h_0	=	impulse response of root-raised cosine filter
TLD	=	tap-delay line
N	=	antenna elements
ULA	=	uniform linear array
UCA	=	uniform circular array
dB	=	decibel
d	=	inter-element spacing [wavelengths]
θ_d	=	desired beam steering direction
AF_{norm}	=	normalized array factor
w_n	=	phase weight vector
n	=	n^{th} antenna elements
$v(\bar{k})$	=	steering vector
$\bar{k}$	=	wave vector in x, y and z direction
k	=	propagation constant [$2\pi/\lambda$]
α_n	=	phase excitation of n^{th} element relative to zero phase
θ_n	=	angular position of n^{th} element on the x-y plane
STC	=	sensitivity time control
R	=	range [metres]
MW	=	mega watts
K	=	kelvin
J	=	joules
deg	=	degree
R	=	range to a target
km	=	kilometers
pW	=	pico watts
PPI	=	plan position indicator
P_{fa}	=	probability of false alarm
P_d	=	probability of detection
TNR	=	threshold-to-noise ratio
T	=	threshold level
P_{noise}	=	noise power
MIMO	=	multiple input multiple output

I. Introduction

A. Motivation

The objective of this paper is to develop and model a radar system in MATLAB using fundamental baseband signal processing and communication techniques. This is to gain a deeper understanding of the operation of radar systems as well as recognize the suitability for applying powerful communication algorithms to radar. While the focus of this paper isn't to explore communication techniques specifically, it will provide a starting point and pathway in which to use these communication techniques to improve radar performance when multiple targets are to be efficiently detected. Powerful multi-user detection techniques from code-division multiple-access have the potential of providing large gains in system performance.

B. Methodology

Prior to commencing any radar modeling, a literature review was undertaken focusing specifically on multiple antenna radars in order to gain an understanding of the radar field and techniques currently being employed. Using this knowledge, a simplistic radar model was developed in the time domain. The focus of this model was to combine fundamental communication processing techniques with known radar techniques such as pulse compression.

The model was reviewed and a more complex radar system model was designed incorporating multiple targets in the time dimension as well as antenna arrays at the transmitter and receiver providing the spatial aspect required for any radar system. The model then underwent a process of validation using realistic radar parameters, leading to the development of a 'Green Screen' user interface, capable of displaying multiple targets in terms of both range and bearing.

II. Background

A. Radar Overview

Radars generally operate by initially transmitting electromagnetic energy through an antenna system in the direction of a desired target. Upon interception of the target, energy is reflected in all directions. Some of this energy, echoed back is directed towards the radar's receiving antenna. The highly sensitive electronics within the receiver analyses the reflected target return and outputs the appropriate range and bearing on the radar display [1].

Two fundamental applications of radar include detection and tracking of targets. In simple terms, detection involves determining whether the received signal at a given instant represents an echo from a reflected object or whether it is simply noise. Moreover, upon detection of an orbject, many radar applications require that the target's position and velocity be tracked. The range from the receiver to the target can be calculated by determining the elapsed time from transmission to detection. Similarly, it is possible to determine the target's elevation ($\emptyset$) and azimuth (θ) angles from knowledge of the antenna's orientation [1]. Moreover, the target's radial velocity can be estimated by measuring the Doppler shift of the target echoes which, when combined with position measurements, can deduce 3D characteristics of the target.

B. Multiple Antenna Radars

1. Phased-Array Radar

A fundamental development in radar theory has been the implementation of the phase-array radar (PAR) with the ability to transmit and/or receive from multiple spatial points. Phased array radars employ multiple antennas co-located at different points, generally with an inter-element spacing of $\lambda/2$ to create a physical aperture [2].

Controlling the relative amplitude and phase of the signal transmitted from each antenna element allows the radiation pattern to be appropriately shaped and the beam pattern to be electronically focused in desired elevation and azimuth directions, without the inertia, time lags and vibrations associated with mechanical rotation [3]. Additionally, rapid beam switching provides the radar system with a greater degree of flexibility to perform multiple radar functions simultaneously.

The generation and distribution of power to these antenna elements can be realised using either passive or active techniques. Implementation of a PAR using passive techniques typically includes the use of a single transmit element for each antenna face. Consequently, the transmitted power is shared among all antenna elements by means of a distributing microwave network. Conversely active array techniques connect each antenna element or group of elements (sub-arrays) to a separate transmission amplifier.

i. Digital Beamforming

In the past, beamforming was restricted to traditional analogue methods which were restricted to producing a single beam at a time. This was insufficient for radar systems that needed to perform multiple functions simultaneously. Digital beamforming, however, allows the formation of multiple, simultaneous beams whilst providing significantly higher dynamic range. Essentially, each antenna element has a delay such that, after this phase adjustment, the wavefront will be aligned across the antenna array. [4].

2. Pulse Compression Radar

Pulse compression radars transmit a long sequence of modulated values which is generally coded using frequency or phase modulation to achieve a larger bandwidth when compared to the bandwidth of the original uncompressed pulse. The received signal is processed with a time delayed version of the transmitted modulation via a pulse compression filter, consisting of a matched filter to achieve maximum SNR followed by a weighting filter if sidelobe levels need to be reduced. Upon correlation, that is correctly matching the two signals, a narrow compressed pulse of maximum amplitude will be achieved [5]. This indicates that the received signal is a delayed and reflected version of the original transmitted pulse. By identifying the time delay that produces this maximum output, the time delay from the radar to the target, and hence the range, can be accurately determined.

III. Simple Radar System Model

In this work, we consider a simple radar system model with three key components: the radar transmitter, the radar channel, and the radar receiver. The following subsections discuss the design of the root-raised cosine filter, radar channel and the system implementation based on Fig. 1.

For simplicity, the transmission signal is composed of a sequence of BPSK modulated symbols {1,-1} oversampled by a factor of 4, prior to filtering. The channel introduces multiple radar returns from targets. These returns are passed through the pulse shaping filter at the receiver and undergo a process of correlation with the originally transmitted sequence. A response is received if the returns are comparably similar to the transmitted signal, which is demonstrated in Section C.

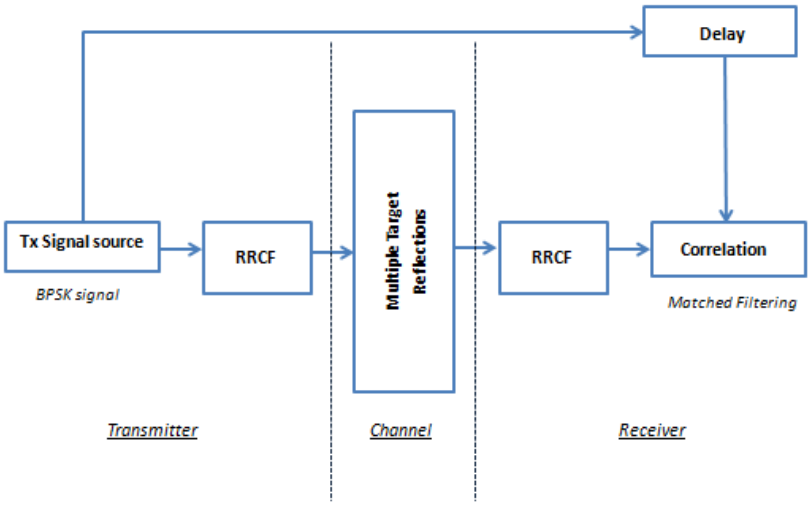

Fig.1: Simplified Radar Block Diagram

A. Design of Root-Raised Cosine Filter

Transmission of a signal over a bandwidth-limited channel can result in the extension and overlapping of adjacent symbols, known as Inter-symbol Interference (ISI). Raised cosine filters (RCF) were designed to avoid this phenomenon by satisfying the Nyquist criterion, effectively suppressing the spectral distortion at integer multiples of the sampling rate [6]. Consequently, placing adjacent pulses at the sampling times produce no ISI.

For simulations, the raised cosine filter was divided into two parts, with a root-raised cosine (RRC) filter located both at the transmitter and receiver. Each filter has the transfer function of the square root of the raised cosine filter function. The key reason for this is together they produce the desired transfer function of the raised cosine filter. The equations outlined below were derived from [6] and subsequently used in MATLAB to design the pulse shaping filter implemented at both the transmitter and receiver. The transfer function of the root-raised cosine filter is shown in Eq. (1) where ω_c , r and T_c represents the corner frequency in radians per second, the roll off factor and chip length respectively.

$$H_{RRC}(\omega) = \begin{cases} B \; for \; |\omega| \leq \omega_1 \\ \frac{B}{\sqrt{2}}\sqrt{1 + cos\left(\pi \frac{|\omega| - \omega_1}{r\omega_c}\right)} \; for \; \omega_1 \leq |\omega| \leq \omega_2 \\ 0 \; for \; |\omega| > \omega_2 \end{cases} \quad (1)$$

$$\omega_1 = \frac{1-r}{2}\omega_c \quad (2)$$

$$B = \sqrt{A} = \sqrt{\frac{2\pi}{\omega_c}} = \sqrt{T_c} \quad (3)$$

Using the derivation in [6], the impulse response, $h_0(t)$ of the root-raised cosine filter is given by Eq. (4).

$$h_0(tT_c) = \frac{sin(\pi t(1-r)) + 4rtcos(\pi t(1+r))}{\pi t(1-(4rt)^2)} \quad (4)$$

The function outlined in Eq. (4) has two removable singularities, resulting in the formation of Eq. (5) and Eq. (6) shown below.

$$At \; t = 0, h_0(0) = 0 \quad (5)$$

$$At \; t = \pm\frac{1}{4r}, h_0\left(\pm\frac{T_c}{4r}\right) = 0 \quad (6)$$

Using L'Hôpital's rule, the function value at the singularities outlined in Eq. (5) and Eq. (6) can be derived according to [6]:

$$For \; t \to 0, h_0(0) = (1-r) + \frac{4r}{\pi} \quad (7)$$

$$For \; t \to \pm\frac{1}{4r}, h_0\left(\pm\frac{T_c}{4r}\right) = \frac{r}{\sqrt{2}}\left(\left(1 + \frac{2}{\pi}\right)sin\left(\frac{\pi}{4r}\right) + \left(1 - \frac{2}{\pi}\right)cos\left(\frac{\pi}{4r}\right)\right) \quad (8)$$

B. Design of Radar Channel

Two approaches to modelling multiple returns from multiple targets have been explored; the first implementation uses a tap delay line (TDL) while the second uses a sparse matrix implementation for realisation. The channel model was introduces as shown in Fig. 1 and simulated both with and without multiple radar reflections.

A TDL channel is well known for its application in mobile radio communications. The received signal is simply the sum of multiple replicas of the transmitted signal due to phenomena such as reflection, scattering and refraction.

The sparse matrix representation consists of a vector of real coefficients on the band diagonal with all remaining entries of the matrix set to zero. The number of coefficients or taps implemented can be manually adjusted depending on the application.

Simulations were independently conducted for each channel and the results were compared to ensure an adequate level of similarity. As expected, the matched filtered response adequately represented the BPSK modulated symbols contained within the original signal.

C. System Implementation

An intermediate step in the design was to simulate the model without multiple target reflections. The random binary bit stream generated was oversampled and convolved with the impulse response of the RRC filter at the transmitter and receiver, with an oversampling factor of 4 and roll of factor of 0.5. Using a matched filter, the received sequence was correlated with the transmitted signal by performing convolution of the received signal with a time delayed version of the transmitted signal. This produced a narrow pulse with maximum amplitude as shown in Fig. 2, identifying that the received signal had similar characteristics to the original signal transmitted.

The next progression outlined in Fig. 1 introduced multiple target modeling. The proximity of a radar target to a radar receiver determines the level of attenuation of the received signal. For simplicity, Fig. 3 identifies three radar reflections simulated at three varying signal power levels.

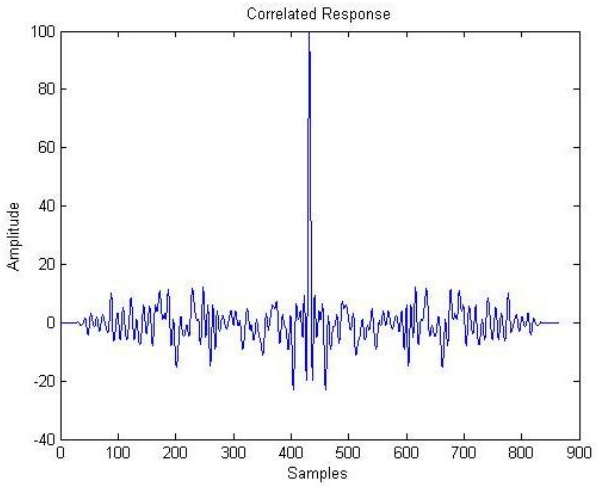

Fig.2: Correlated Response

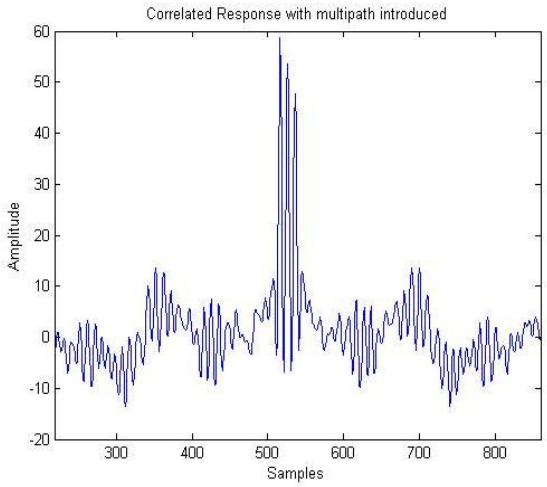

Fig.3: Correlated Response with Multiple Target Returns

IV. Complete Radar System Model

The complete radar system block diagram is depicted in Fig. 4, incorporating a spatial dimension to the radar system model proposed in Fig. 1. This was achieved through the implementation of antenna arrays at both the transmitter and receiver. Additionally, development of a 'Green Screen' user interface provides a display option for multiple targets in terms of range and bearing.

The random BPSK modulated signal is transmitted via an N element uniform linear array (ULA) antenna or N element uniform circular array (UCA) antenna depending upon the application. Phase shifts are applied to each antenna element such that the resulting antenna beam will be steered at 1 degree increments in the azimuth direction. After this point, random noise is added to the radar channel and the SNR is determined. Realistic modeling of Fig. 4 required consideration of actual radar parameters, such as transmission power, antenna gain, noise figure and radar cross section. Additionally, 11dB of system losses were incorporated into the model, simulating the losses associated with each stage of signal processing.

The resulting signal is received by a ULA or UCA antenna which produces the conjugate of the array factor generated at the transmitter. Summation of the received signal from each of the antenna elements is followed by processing with a time delayed version of the transmitted signal via a pulse compression filter. The pulse compression filter consists of a matched filter, designed to recognise the characteristics of the transmitted pulse as they arrive at the receiver in the form of reflections [1]. This is equivalent to convolving the unknown received signal with a time-reversed version of the original signal transmitted. When a waveform with similar characteristics to the transmitted waveform is passed through the matching pulse-compression filter [1], a narrow compressed pulse of maximum amplitude is achieved. This is also similar to a CDMA despreading operation, where the bit energy of the symbols is recovered from the spread sequence.

Lastly, a threshold level is chosen such that radar returns above this predefined threshold appear as targets on the plan position indicator (PPI) display, while returns failing to meet this level are classified as missed detections. The key reason for the implementation of the PPI display was its map-like representation of radar returns in terms of their polar coordinates. As shown in Fig. 14, the associated range to the target is represented by the radial displacement of the blip from the centre of the display and the target's azimuth angle is represented by the angle of the radius vector measured anticlockwise from 0 degrees.

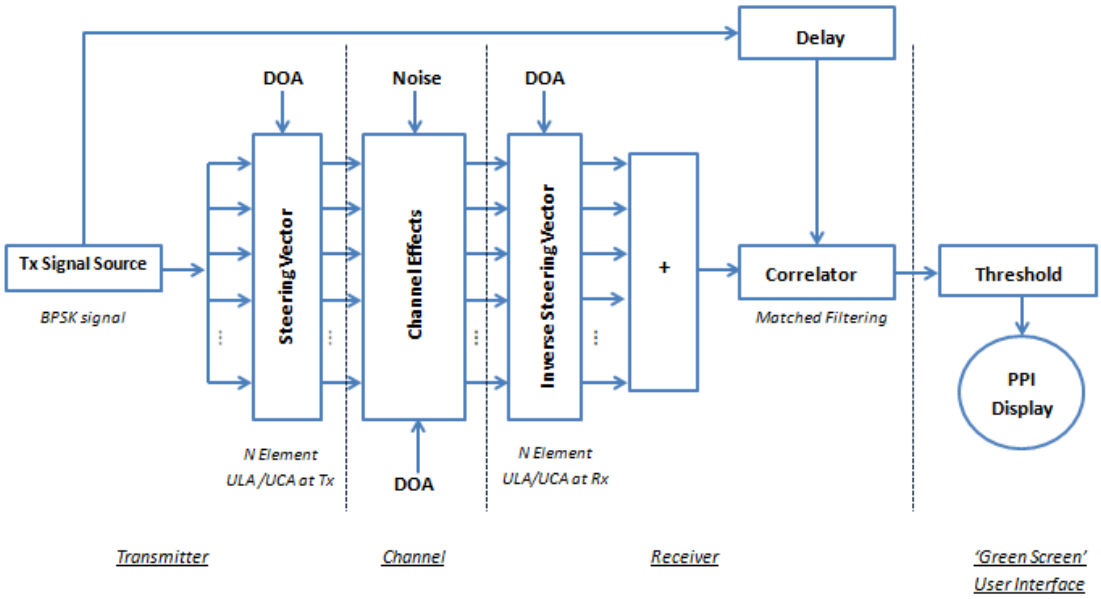

Fig.4: Radar Block Diagram

A. Design of Uniform Linear Array Antenna

Antenna arrays are being actively used to achieve increases in both antenna gain and directivity. Transmission of a phase-shifted carrier from each of the antenna array elements causes the radiated fields to reinforce in some directions and destructively interfere in the remaining directions. A uniform linear array (ULA) antenna is depicted in Fig. 5 and implemented to achieve radiation patterns that could be steered in a desired direction without the need to physically change the orientation of the individual antenna elements.

For simplicity, the N element ULA has elements aligned along the z-axis, with an inter-element spacing of $d = \lambda/2$, where λ represents wavelength in metres. There are however limitations on the element spacing which is usually restricted to a maximum of λ/2 to avoid the effects of grating lobes. Grating lobes are undesirable as they steel power from the main beam and lead to the creation of additional beams, replicating the main beam pattern in unwanted directions. These replicated beams can produce false target generation and lead to interference with nearby radar systems.

The radiation pattern of an array depends heavily on the weighting method employed and the geometry of the array. In order to alter the direction in which the array is steered, application of a linear phase taper to the weights is required to compensate for the phase delay associated with the propagation of the signal in the desired direction, θ_d.

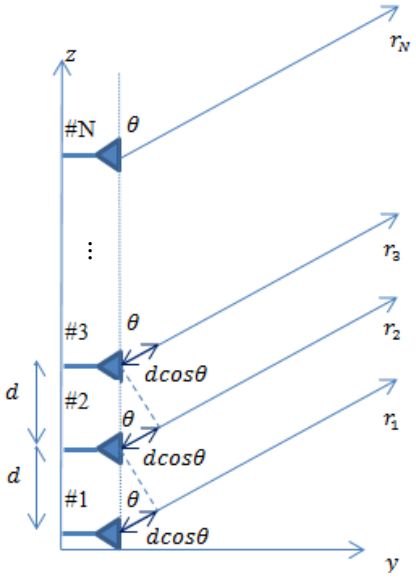

Fig.5: Uniform Linear Array Antenna

Assuming constant elevation (∅=90 degrees), the normalized array factor, AF_{norm} can be written in terms of the phase weight vector, w_n for the n^{th} element and the steering vector $v(\bar{k})$; vector of propagation delays across an array for a given wave vector, $\bar{k}$.

$$w_n = e^{jkndcos\theta_d} \tag{9}$$

$$v(k) = e^{-jkndcos\theta} \tag{10}$$

$$AF_{norm} = \frac{1}{N}\sum_{n=0}^{N-1} {w_n}^T v(\bar{k}) \tag{11}$$

$$AF_{norm} = \frac{1}{N}\sum_{n=0}^{N-1} e^{jnkd(cos\theta_d - cos\theta)} \tag{12}$$

Using the identity outlined in Eq. (13), the AF_{norm} can be further derived into Eq. (14).

$$\sum_{n=0}^{N-1} c^n = \frac{c^N - 1}{c - 1} \tag{13}$$

$$AF_{norm} = \frac{1}{N} \frac{sin\,[\frac{kdN}{2}(cos\theta_d - cos\theta)]}{sin\,[\frac{kd}{2}(cos\theta_d - cos\theta)]} \tag{14}$$

Unfortunately, there is a beamsteering disadvantage associated with this antenna configuration. The beamsteering capability becomes ambiguous beyond 180 degrees and is generally restricted to 120 degrees [7]. This is a result of applying small phase variations to each element, consequently directing the main beam at an angle dependent upon the phase shift applied. Beyond 60 degrees either side of boresight, the effective area of the antenna in the direction of the beam is reduced, producing a broad main beam pattern with obvious reductions in gain and resolution [1].

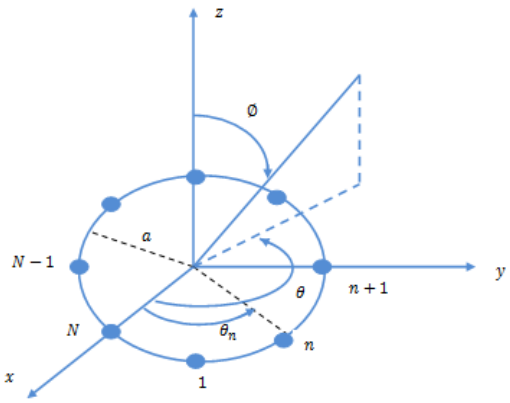

Fig.6: Uniform Linear Array Antenna

B. Design of Uniform Circular Array Antenna

Due to the beamsteering limitations of a ULA antenna, a uniform circular array (UCA) antenna was considered. The standard arrangement is shown in Fig. 6. This configuration has the ability to scan 360 degrees in azimuth with no distortions near the end-fire directions, as experienced with a ULA antenna. Using the derivations outlined in [8], the normalized array factor of N equispaced elements with constant elevation (∅=90 degrees) can be written as

$$AF_{norm} = \frac{1}{N} \sum_{n=0}^{N-1} e^{j[ka\,cos(\theta - \theta_n) + \alpha_n]} \tag{15}$$

Where a represents the radius of the circular array, α_n is the phase of the excitation of the n^{th} element relative to a chosen array element of zero phase and $\theta_n = \frac{2\pi n}{N}$ represents the angular position of the n^{th} element on the x-y plane.

According to [8], in order to direct the peak of the main beam in a desired azimuth direction θ_d the phase of the n^{th} element can be written as

$$\alpha_n = kacos\,(\theta_d - \theta_n) \tag{16}$$

Substitution of Eq. (16) into Eq. (15) produces the normalized array factor outlined in Eq. (17) below

$$AF_{norm} = \frac{1}{N} \sum_{n=0}^{N-1} e^{jka[cos(\theta - \theta_n) - cos\,(\theta_d - \theta_n)]} \tag{17}$$

Unlike the ULA antenna, the angular resolution of a UCA antenna is reasonably well maintained over the full 360 degrees of azimuth coverage. Additionally, as a result of a high degree of symmetry, the UCA antenna is able to provide relatively identical beam shapes in all azimuth direction. A comparison between a ULA antenna and UCA antenna at the same azimuth angle is shown in Fig. 7 and Fig. 8 respectively. Unlike the UCA antenna, the beamwidth of the ULA antenna varies in addition to fluctuations in sidelobe power and direction.

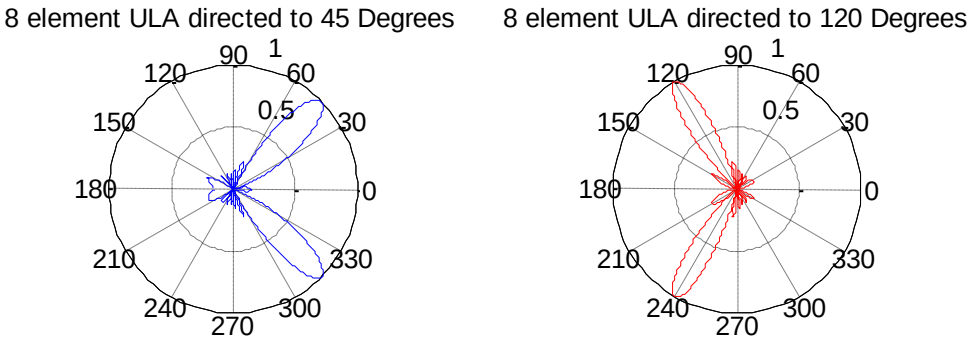

Fig.7: Radiation Pattern for ULA Antenna

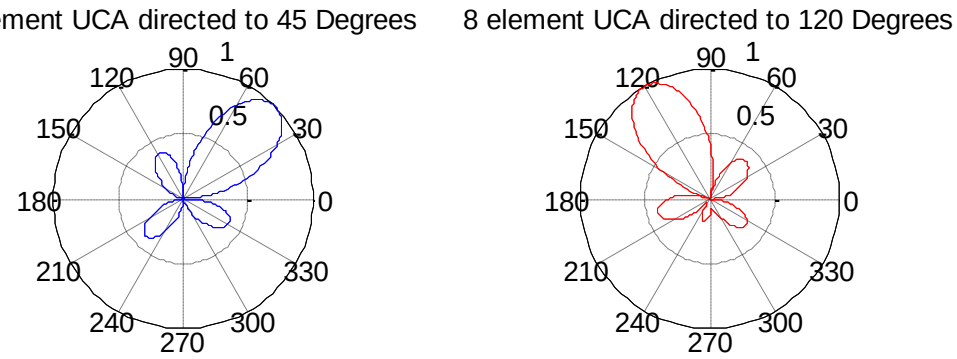

Fig.8: Radiation Pattern for UCA Antenna

C. Sensitivity Time Control

The path loss experienced by radar returns arriving at the radar receiver results in rather broad variations in signal amplitude. There are a number of techniques utilized to adjust the receiver gain. The objective of sensitivity time control (STC) is to control receiver gain by gradually modifying the gain of the amplifier as a function of time. A generalised concept is illustrated in Fig. 9. At the transmission of a waveform, the receiver gain is minimised and then gradually increased to a maximum just prior to the transmission of the next waveform. Ideally, the gain would increase proportional to R^4 as demonstrated by the radar range equation, and not linearly as a function of time.

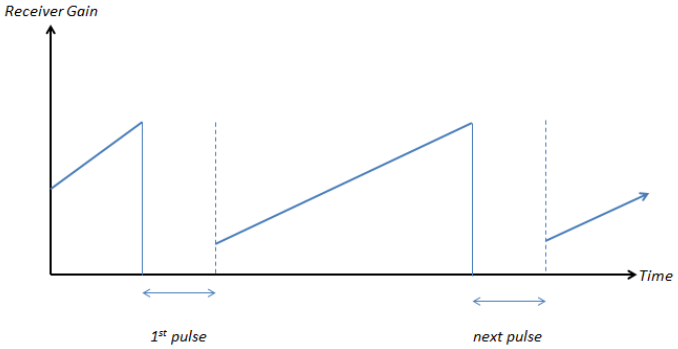

Fig.9: Generalised Concept of Sensitivity Time Control [1]

Radar and clutter returns in close proximity to the radar receiver already have sufficient energy, thus, require less gain for processing. Conversely, radar and clutter returns furthest from the radar receiver require a greater level of amplification. These returns lack sufficient energy to be processed without any gain adjustment [1]. This technique is implemented in the following simulations.

D. System Implementation

In this work, we consider the radar system model depicted in Fig. 4, where conventional radar parameters are utilised in a number of scenarios. The radar system is simulated where the radar is on a ship out at sea, detecting stationary airborne targets at a constant elevation. The simulation parameters are detailed in Table 1 where the transmission gain, antenna gain, system losses, noise figure, radar cross section and noise temperature are listed.

The parameters are typical values used by surveillance radars. To better predict radar performance, system losses were incorporated into the simulations. A combined loss of 11-12dB is attributed to plumbing loss (approx. 3dB), beam-shape loss (approx. 3dB), field degradation (approx. 3 dB) and loss associated with the use of non-ideal equipment (2dB) [9]. Using [1] and [9], the noise figure of a radar receiver is typically between 8 and 10dB.

Table 1: Simulation Parameters for Radar System Model

Transmit Power	60 dBW (1MW)
Antenna Gain (Tx and Rx)	38 dB
System Losses	11 dB
Noise Figure	8 dB
Radar Cross Section	6 dB (3.98 m^2)
Boltzman's Constant	$1.38x10^{-23}Jdeg^{-1}$
Noise Temperature of Rx	290K

Radar cross section values can be as small as $0.01m^2$ for a cruise missile and small birds or $100m^2$ for large commercial aircraft [10]. Simulations were conducting assuming targets were small or large fighter aircraft (2-$3m^2$ and 4-$6m^2$ respectively) [11]. A noise temperature of 290K was chosen, coinciding with a conventional radar system. The parameters can be modified within MATLAB to simulate a given environment or scenario.

Using a pulse compression approach, a random binary bit stream is transmitted with 60dBW of power from an antenna array with a 38dB antenna gain. The antenna array consists of 5 uniformly spaced elements for a ULA antenna or 8 equispaced elements for a UCA antenna. The antenna is swept through an azimuth of 180 degrees or 360 degrees (depending upon the antenna configuration) through the introduction of phase shifts,

effectively scanning the beam at 1 degree increments in azimuth. Random noise is added to the channel and the path loss and SNR is calculated. The channel introduces returns from targets when the incident energy intercepts the target as is reflected back towards the radar receiver. These returns are correlated using a pulse compression filter. The correlation results are plotted in Fig.10 and Fig. 11 and briefly discussed for two radar scenarios.

E. Simulation Results

In this section we consider simulation results for two separate, stationary, multiple target radar scenarios assuming constant target elevation. Fig. 10 shows the correlated output response after the application of pulse compression for three radar targets spatially located at 60 degrees in azimuth with three distinct ranges. The three targets are located at times 120us, 124us and 128us respectively. As expected, the upper subplot of Fig. 10 shows that increasing the range of targets from the radar receiver reduces the received power level at the receiver. This behavior coincides with the radar range equation, which illustrates that received power is proportional to the fourth power of the distance of a target from the radar receiver.

Fig.10: Received Power of Radar Returns as a Function of Time without (top) STC and with (below) STC

In order to reduce the power of the strongest target reflection (tallest spike at time 120 us) and subsequently increase the power of the two weaker target reflections, STC was applied by multiplying the correlated output response with the path loss curve reflected about the x-axis (range). The very weak amplification at the beginning of the receive stage has reduced the strongest target reflection. Similarly, the strong amplification at the end of the receive stage has effectively increased the weaker target reflections [1]. The result is shown in the bottom subplot of Fig. 10 which depicts three target returns that are now easily depicted above the noise and closely aligned in terms of received power. Noticeably, the receive power after STC is much lower. However, this is a relative level as it is dependent upon the exact values used within the calculation of the path loss curve.

In the second scenario, the three radar targets have kept the same range as previously simulated, however, are now positioned at three separate spatial locations, 30 degrees, 40 degrees and 45 degrees. Again, using a pulse compression approach, the antenna beam is swept in azimuth over 360 degrees and radar reflections from each of the three targets are analysed. In Fig. 11 the correlated output response is shown when the antenna is directly pointed at the second target.

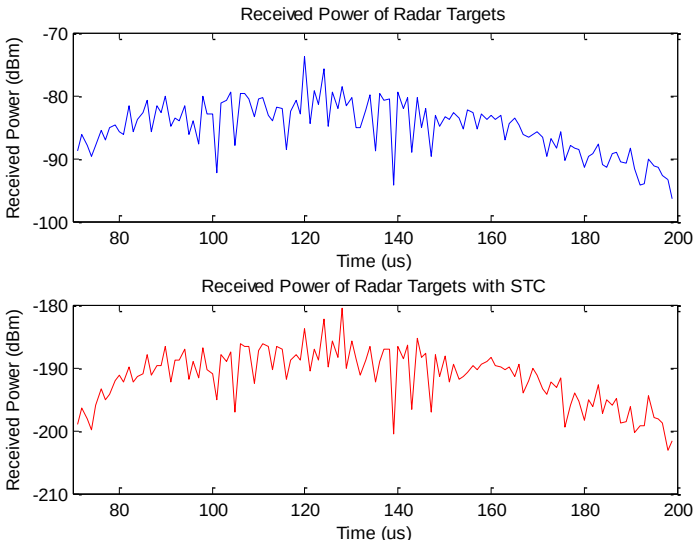

Fig.11: Received Power of Radar Returns as a Function of Time without (top) STC and with (below) STC

Once again, Fig. 11 agrees with the radar range equation highlighting higher received power levels for targets that are closest to the receiver (tallest spike at time 120us). Whilst the third target (small spike at time 128us) is quite difficult to distinguish above the noise in the upper subplot of Fig. 11, after applying STC, all three targets are now easily differentiated from the corresponding noise as highlighted in the bottom subplot of Fig. 11. It can be easily seen that the power level for each target reflection has been reduced. However, this relative level is still acceptable considering the highly sensitive receiver electronics.

Furthermore, normalization of the noise ensured the noise floor was

relatively constant and a threshold value could be selected above this level, such that radar returns surpassing this threshold level could be displayed on the user interface developed. The result of the normalisation for both radar scenarios is shown in Fig. 12 and Fig. 13 respectively. Again it can be easily seen that the power levels of each target reflection exceeds the threshold level selected in both radar scenarios. Additionally, at certain time instances, the noise is bordering on or close to exceeding this threshold level. If the noise was to exceed this level, we would see additional targets displayed on the plan position indicator (PPI) corresponding to false target detections.

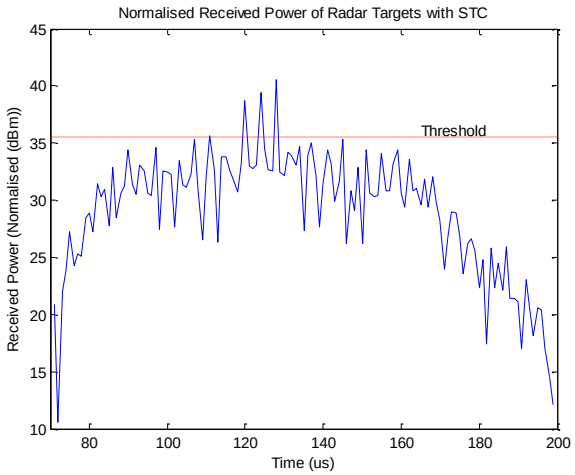

Fig.12: Normalised Received Power of Radar Returns as a Function of Time (Radar Scenario One)

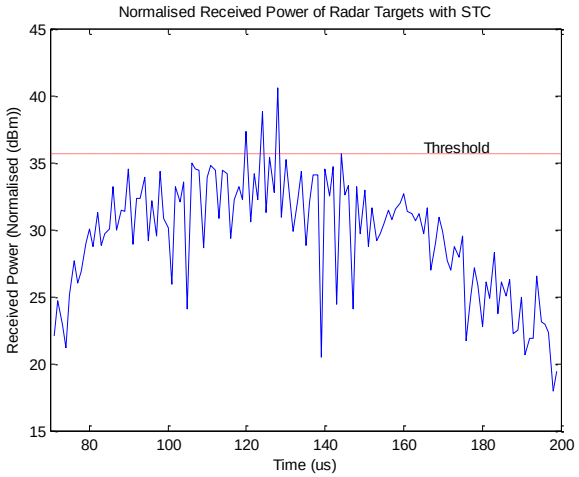

Fig.13: Normalised Received Power of Radar Returns as a Function of Time (Radar Scenario Two)

Selection of a threshold involved analysis of the tradeoffs between probability of false alarm (P_{fa}) and probability of detection (P_d). Ideally, a threshold would be chosen such that the $P_{fa}$is minimised to zero while the P_d maximized. Unfortunately, reducing P_{fa} additionally results in unwanted reductions in P_d. As such, a compromise was made between the two functions.

A common method employed is to select a threshold level based on a specific probability of false alarm, in this case 10e-5 (one false alarm every 100,000 samples) was chosen. After which, the threshold to noise ratio (TNR) could be derived according to [12] and the threshold level, represented by the red dotted line in Fig.12 and Fig. 13, could be incorporated into the simulations.

The probability of false alarm can be written as

$$P_{fa} = P(x \geq T) = \int_T^{\infty} \frac{1}{N} e^{-\frac{x}{N}} dx = e^{-\frac{T}{N}} \tag{18}$$

Where T represents the threshold level and P_{noise} represents the noise power. Therefore, after simple manipulation, the TNR is represented by Eq. (19) and the threshold level can be redefined according to Eq. (20).

$$TNR = \frac{T}{N} = -ln\,(P_{fa}) \tag{19}$$

$$T = \sqrt{TNR \times P_{noise}} \tag{20}$$

Once the threshold level was selected, target returns arriving at the radar receiver exceeding this level were displayed on the PPI display shown in Fig. 14. In this simulation, we uniquely limited the number of stationary radar targets and fixed their range and bearing in order to analyse the detection performance of the radar model developed.

A validation process was performed to ensure that all targets were correctly identified, and were not false target generations produced from noise or clutter exceeding the threshold level. The results have highlighted six out of six possible targets exceeding the defined threshold level. Each target is displayed as a red 'x' on the PPI display shown in Fig. 14. The PPI display essentially links the major radar functions within Fig. 4 into a real time display. Due to the volume of simulations required and time constraints, a statistical analysis on $P_{fa}$and P_d was not performed in this paper.

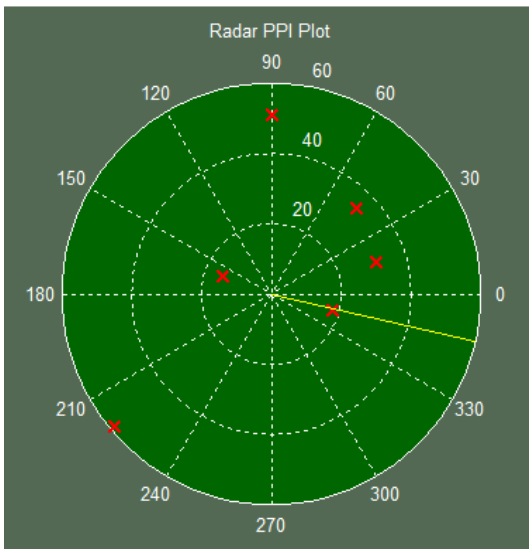

Fig.14: 'Green Screen' User Interface

V. Conclusions

In this paper we have explained the development and implementation of a radar system model in MATLAB in both time and spatial dimensions. The focus has very much been tailored towards understanding the system model, validating fundamental digital signal processing techniques and demonstrating how they can be applied to a theoretical radar system.

Specifically, it has detailed the design and properties of the root-raised cosine filtering method to avoid the phenomena known as Intersymbol Interference (ISI). This paper also discusses the design of a basic radar model simulating multiple target reflections through two unique channel model implementations.

Development of these techniques has resulted in the design of a baseband model of a radar system in MATLAB which is capable of identifying targets in terms of both range and azimuth and consequently displaying them on a 'Green Screen' user interface. This model can be implemented with either a ULA antenna or UCA antenna depending upon the application and the azimuth coverage required. A matched filter is integrated into the model to recognise the presence of radar reflections arriving at the receiver that have similar characteristics to the original signal transmitted.

From the results obtained, we are in a good position to consider applying powerful multi-user detection techniques from communication systems to improve the radar system performance.

VI. Recommendations

This report has been motivated by considering the similarities between a communication system and a radar system. Since the design and development of a radar system model has been implemented, the next progression is the application of communication techniques, specifically CDMA and multiuser detection to this framework.

Due to the commercial success of CDMA in mobile cellular systems [13], there has been a lot of research in multiuser detection, whereby a receiver can simultaneously detect multiple transmission paths, in addition the channel models and receiver techniques used with multiple input multiple output (MIMO) [14] could also potentially be adopted. In the same way that multiuser detection uses an estimate for the interference and progressively subtracts this estimate from the received composite signal to improve the reception of the remaining mobile users, this concept can likewise be applied to multiple target detection in radar. A single radar receiver capable of detecting multiple target returns simultaneously has the potential for significant performance advantages. We expect that using multiuser detection techniques, an estimate for a target can be subtracted from the remaining composite echo signal to not only detect but also improve the reception of the remaining targets.

Acknowledgements

I would like to thank my thesis supervisor, Dr Mark Reed for his guidance, mentorship and for opening my eyes to the possibility of further studies.

References

[1] I. Faulconbridge, Radar Fundamentals, Canberra: Argos Press, 2002.

[2] A. Farina, “Introduction to Radar Signal and Data Processing: The Opportunity,” NATO OTAN, Rome, 2006.

[3] S. Nitschke, “Active and Passive Phased Array Radars Compared,” *Naval Technology,* vol. 2, pp. 68-73, 2007.

[4] M. Parker, "Radar Basics - Part 3: Beamforming and radar digital processing," Altera Corporation, 2011.

[5] J.R.Klauder, A. C. Price, S. Darlington and W. J. Albersheim, “The Theory and Design of Chirp Radars,” *The Bell System Technical Journal,* vol. XXXIX, no. 4, pp. 745-751, 1960.

[6] M. Joost, “Theory of Root-Raised Cosine Filter,” Research and Development, Krefled, Germany, 2010.

[7] B. Allen and M. Ghavami, Adaptive Array Systems: Fundamentals and Applications, John Wiley and Sons, 2006.

[8] R. Zekavat and R. M. Buehrer, Handbook of Position Location: Theory, Practice and Advances, John Wile and Sons, 2011.

[9] M. I. Skolnik, Introduction to Radar Systems, New Yorlk: McGraw Hill Book Company, Inc, 1962.

[10] M. C. Rezende, I. M. Martin and R. Faez, “Radar Cross Section measurements (8-12 GHz) of Magnetic and Dielectric Microwave Absorbing Thin Sheets,” *Revista de Fisica Aplicada e Instrumentaccao,* vol. 15, no. 1, p. 24, 2002.

[11] R. A. Stonier, “Stealth aircraft and Technology From World War II to the Gulf. Part II: Applications and Design,” *SAMPE Journal,* vol. 27, no. 5, 1991.

[12] J. M.C. Budge, “Detection Theory,” ECE Department, University of Alabama, Huntsville, 2011.

[13] M. L. Honig and R. Ratasuk, “Large-system performance of iterative multiuser decision-feedback detection,” *IEEE Transactions on Communications,* vol. 51, no. 8, pp. 1368-1377, 2003.

[14] M. Garg, “Multi-user Detection,” Indian Institute of Technology, Bombay, 2005.

[15] W. L. Melvin, "A STAP Overview," *IEEE Aerospace Electromagnetic Systems Magazine,* vol. 19, no. 1, pp. 19-35, 2004.

[16] R. Klemm, *Principles of Space-Time Adaptive Radars,* Jerts: UK: Institute of Electrical Engineers (IEE Press), 2002.

[17] H. Commin, “Spatiotemporal Arrayed MIMO Radar,” Department of Electrical and Electronic Engineering, Imperial College London, London, 2013.

[18] A. Hassanien and S. A. Vorobyov, "Phased-MIMO Radar: A Tradeoff between Phased-Array and MIMO Radars," *IEEE Transactions on Signal Processing,* vol. 58, no. 6, pp. 3137-3151, 2010.

[19] A. M. Haimovich, R. S. Blum and L. J. Cimini, "MIMO Radar with Widely Separated Antennas," *IEEE Signal Processing,* pp. 116-129, January 2008.

[20] L.Yang, “The Applicability of the Tap-Delay Line Channel Model to Ultra Wideband,” Virginia Polytechnic Institute and State University, Blacksburg, 2004.

[21] “Chapter 10,” in *Pulse Compression,* Argos Press, pp. 133-138.

[22] Balanis, "Lecture 18: Planar Arrays, Circular Arrays," [Online]. Available: http://www2.elo.utfsm.cl/~elo352/biblio/antenas/Lectura%2018.pdf. [Accessed 12 September 2014].

[23] H. Commin, *Spatiotemporal Arrayed MIMO Radar,* Imperial College London: Department of Electrical and Electronic Engineering, 2013.